

UC Berkeley

UC Berkeley Previously Published Works

Title

The Transcriptome and Flux Profiling of Crabtree-Negative Hydroxy Acid-Producing Strains of *Saccharomyces cerevisiae* Reveals Changes in the Central Carbon Metabolism

Permalink

<https://escholarship.org/uc/item/1ck4h3m0>

Journal

Biotechnology Journal, 14(9)

ISSN

1860-6768

Authors

Jessop-Fabre, Mathew M

Dahlin, Jonathan

Biron, Mathias B

et al.

Publication Date

2019-09-01

DOI

10.1002/biot.201900013

Peer reviewed

The Transcriptome and Flux Profiling of Crabtree-Negative Hydroxy Acid-Producing Strains of *Saccharomyces cerevisiae* Reveals Changes in the Central Carbon Metabolism

Mathew M. Jessop-Fabre, Jonathan Dahlin, Mathias B. Biron, Vratislav Stovicek, Birgitta E. Ebert, Lars M. Blank, Itay Budin, Jay D. Keasling, and Irina Borodina*

Saccharomyces cerevisiae (*S. cerevisiae*) is the yeast cell factory of choice for the production of many biobased chemicals. However, it is a Crabtree-positive yeast and so shuttles a large portion of carbon into ethanol. Ethanol formation can be eliminated by deleting pyruvate decarboxylase (PDC) activity. It is not yet well understood how PDC-negative yeasts are affected when engineered to produce other products than ethanol. In this study, pathways are introduced for the production of three hydroxy acids (lactic, malic, or 3-hydroxypropionic acid [3HP]) into an evolved PDC-negative strain. These strains are characterized via transcriptome and flux profiling to elucidate the effects that the production of these hydroxy acids has on the host strain. Expression of lactic and malic acid biosynthesis pathways improved the maximum specific growth rate (μ_{max}) of the strain by 64% and 20%, respectively, presumably due to nicotinamide adenine dinucleotide regeneration. All strains show a very high flux (> 90% of glucose uptake) into the oxidative pentose phosphate pathway under batch fermentation conditions. The study, for the first time, directly compares the flux and transcriptome profiles of several hydroxy acid-producing strains of an evolved PDC-negative *S. cerevisiae* and suggests directions for future metabolic engineering.

1. Introduction

Saccharomyces cerevisiae (*S. cerevisiae*) has long been used as a production organism for ethanol and more recently for other biochemicals and recombinant proteins. When grown on high concentrations of glucose, yeast ferments and produces ethanol even in abundant oxygen conditions.^[1] This is known as the Crabtree effect, and while such a trait has proven useful for ethanol fermentation, the alcohol is an unwanted by-product in the biobased production of many other chemicals.^[2–4] Under fermentative growth on glucose, a large fraction of the flux from pyruvate passes through the three main pyruvate decarboxylases (PDCs) to be converted into acetaldehyde, which is, in turn, reduced to ethanol via alcohol dehydrogenases (ADH), with Adh1p as the major ADH isozyme.^[5] PDC activity is

Dr. M. M. Jessop-Fabre, J. Dahlin, M. B. Biron, Dr. V. Stovicek, Prof. J. D. Keasling, Dr. I. Borodina
The Novo Nordisk Foundation for Biosustainability
Technical University of Denmark
Building 220
2800, Kongens Lyngby, Denmark
E-mail: irbo@biosustain.dtu.dk

Dr. B. E. Ebert, Prof. L. M. Blank
Institute of Applied Microbiology
RWTH Aachen University
Worringer Weg 1
52074, Aachen, Germany


Prof. J. D. Keasling
Joint BioEnergy Institute
Emeryville, CA 94608, USA

Prof. J. D. Keasling
Biological Systems & Engineering Division
Lawrence Berkeley National Laboratory
Berkeley, CA 94720, USA

Dr. I. Budin, Prof. J. D. Keasling
Department of Chemical and Biomolecular Engineering
University of California
Berkeley, CA 94720, USA

Dr. I. Budin, Prof. J. D. Keasling
Department of Bioengineering
University of California
Berkeley, CA 94720, USA

Prof. J. D. Keasling
Center for Synthetic Biochemistry, Institute for Synthetic Biology
Shenzhen Institutes for Advanced Technologies
Shenzhen 518055, China

 The ORCID identification number(s) for the author(s) of this article can be found under <https://doi.org/10.1002/biot.201900013>.

© 2019 The Authors. *Biotechnology Journal* Published by Wiley-VCH Verlag GmbH & Co. KGaA, Weinheim This is an open access article under the terms of the Creative Commons Attribution License, which permits use, distribution and reproduction in any medium, provided the original work is properly cited.

DOI: 10.1002/biot.201900013

conferred through the three major PDC isozymes: Pdc1p, Pdc5p, and Pdc6p.^[6–8] One successful strategy for the removal of ethanol formation has been to eliminate pyruvate flux into acetaldehyde by deleting all three major PDC isozymes.^[4,9] Such a PDC-negative strain is hypersensitive to glucose and cannot grow on high concentrations of glucose without the addition of a C2 compound such as ethanol or acetate.^[10] The growth defect is caused by a redox cofactor imbalance, where nicotinamide adenine dinucleotide (NADH) generated during glycolysis can no longer be oxidized during ethanol formation, and by the lack of cytosolic acetyl-CoA, which is synthesized from acetaldehyde via acetate. Previously, the directed evolution of a PDC-negative strain eliminated its dependency on C2 compounds and greatly improved its glucose tolerance and growth characteristics.^[11] While some of the wild-type (WT) growth characteristics were rescued, the resulting strain (referred to as the TAM strain) still has a much slower growth rate than WT; 0.20 h⁻¹ versus 0.33 h⁻¹.^[11] The genome of the TAM strain was later sequenced, revealing that much of the observed phenotype was due to a large deletion in the glucose-sensing transcriptional regulator *MTH1*.^[12] This deletion is hypothesized to reduce the degradation rate of Mth1p. Mth1p reduces the expression of hexose kinase-coding genes and slows down glucose uptake rate, which, in turn, reduces the redox cofactor imbalance caused by NADH generation during glycolysis.^[12] The reduction in glucose uptake presumably also leads to derepression of the *ACH1* gene, encoding a mitochondrial protein with CoA-transferase activity. Ach1p generates acetate from acetyl-CoA in mitochondria. Acetate can cross the mitochondrial membrane to enter the cytosol, where it is activated into acetyl-CoA, providing this compound that is essential for cell growth. The TAM strain is a pyruvate overproducer and an attractive host for the production of

pyruvate-derived chemicals, such as industrially important hydroxy acids: malic, lactic, and 3-hydroxypropionic acids (3HPs).^[11,13–16] In the present study, we characterized these three different hydroxy acid production pathways and the impact of the added pathways on the metabolism and physiology of the host TAM strain.

Lactic acid, a three-carbon α -hydroxy acid, can be produced from pyruvate in a single enzymatic step by lactate dehydrogenase (LDH) with NADH as the cofactor. This enzyme, most commonly taken from *Lactobacillus* origin, has been shown to produce high levels of lactate in both PDC-positive and -negative *S. cerevisiae* strains.^[13,17–20] The TAM strain has a redox imbalance due to NAD⁺ not being regenerated through the formation of ethanol. The addition of the *Lactobacillus plantarum* (*L. plantarum*) *ldh1* gene in a PDC-negative strain can provide the cell with NAD⁺, rebalancing the redox state of the cell (**Figure 1**). However, this redox balancing has been shown to be not able to recover anaerobic growth, with lactic acid production being highly dependent on oxygen availability.^[18] Lactic acid transport, unlike ethanol, is assumed to be dependent on adenosine triphosphate (ATP) and is less efficient under anaerobic conditions where ATP production is limited.^[18,21]

High levels of malic acid, a four-carbon α -hydroxy acid, can be produced by overexpression of three genes. The overexpression of the native pyruvate carboxylase gene *PYC1*, the native NADH-dependent malate dehydrogenase *MDH3* lacking the peroxisomal targeting sequence,^[22] and the malate transporter (MAE) from *Schizosaccharomyces pombe* (*S. pombe*) *MAE1*, allows for high malate titers when expressed in the TAM strain, of up to 59 g L⁻¹.^[16] This pathway also regenerates NAD⁺, but is more energetically demanding than the lactic acid pathway because, in addition to the ATP required for malic acid

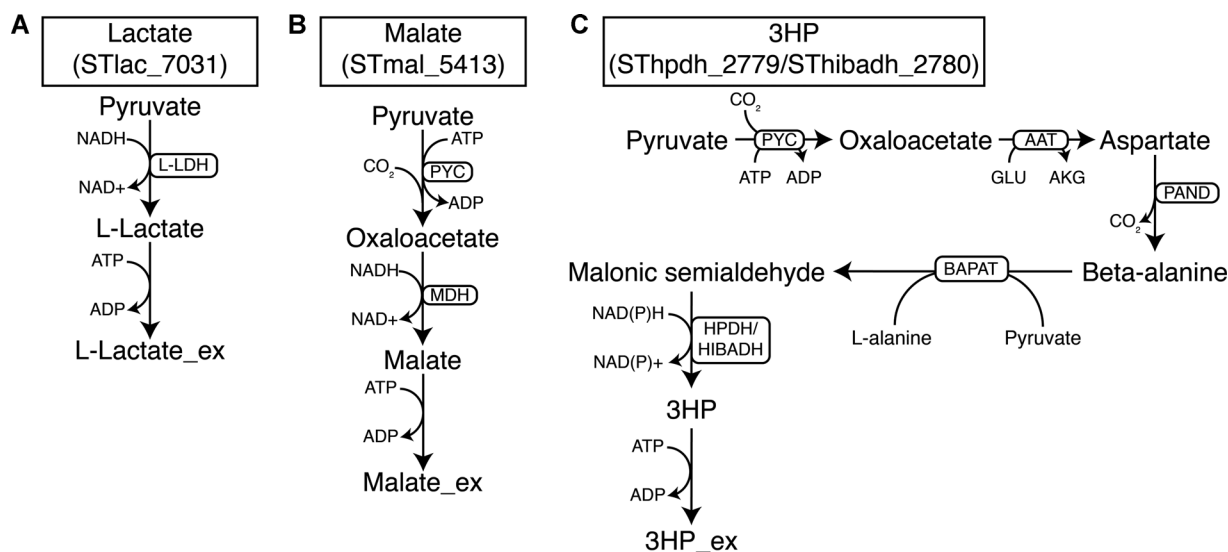


Figure 1. Metabolic routes for the production of three different hydroxy acids in Crabtree-negative *S. cerevisiae*. A) Lactate, B) malate, and C) 3HP are produced from pyruvate in the PDC-negative, pyruvate-overproducing host strain (TAM strain—STtam_2803) through the implementation of heterologous pathways. Enzyme abbreviations: AAT, aspartate amino transferase; BAPAT, β -alanine-pyruvate amino transferase; HIBADH, 3-hydroxyisobuturate dehydrogenase (NADH-dependent); HPDH, 3-hydroxypropionic acid dehydrogenase (NADPH-dependent); L-LDH, L-lactate dehydrogenase; MAE, malate transporter; MDH, malate dehydrogenase; PAND, aspartate decarboxylase; PYC, pyruvate carboxylase. Metabolite abbreviations: 3HP, 3-hydroxypropionic acid. Details about strain construction can be found in Section 2 of this article.

export, ATP is also used for the carboxylation of pyruvate into oxaloacetate.^[14,23,24] The export energetics are also different between monocarboxylic and dicarboxylic acids, and export of malic acid may have a greater total ATP requirement than lactic acid export.^[14] Addition of calcium carbonate has been shown to greatly increase malate titers through its ability to prevent product inhibition.^[25]

The three-carbon β -hydroxy acid, 3HP, can be produced via β -alanine—a pathway identified as having a high potential for 3HP production.^[26] This pathway in a PDC-positive *S. cerevisiae* strain showed titers close to 14 g L^{-1} in controlled bioreactor fermentations.^[15] Five enzymatic steps are required to produce 3HP from pyruvate, three of which require heterologous genes (Figure 1). The final step in this pathway, the conversion of malonic semialdehyde into 3HP, can be performed either by a 3-hydroxyisobutyrate dehydrogenase (HIBADH) that uses NADH as a cofactor or a 3-hydroxypropionate dehydrogenase (HPDH) that uses nicotinamide adenine dinucleotide phosphate (NADPH). In this study, we compared both the HIBADH- and HPDH-based pathways for 3HP biosynthesis.

2. Experimental Section

2.1. Strains

Escherichia coli (*E. coli*) DH5 α was used to clone, propagate, and store the plasmids. A derivative of *S. cerevisiae* strain CEN.PK, the TAM strain, was a kind gift from Prof. Jack Pronk and was used as the host strain for the hydroxy acid production strains (Delft Technical University, Holland). A description of each strain used in this study is shown in Table 1. For the respiration experiments, the CEN.PK113-7D PDC-positive strain (*MATa URA3 HIS3 LEU2 TRP1 MAL2-8c SUC2*) was used as a reference. This was a kind gift from Peter Kötter, Johann Wolfgang Goethe University, Frankfurt, Germany.

2.2. Plasmid Construction and Yeast Transformation

Each of the plasmids (Table S2, Supporting Information) used to create the hydroxy acid-producing strains (Table S3, Supporting Information) were constructed using the EasyClone vector set for chromosomal gene integrations with auxotrophic

selection markers as described in Jensen et al.^[27] Yeast promoter biobricks were amplified from the genomic DNA of CEN.PK113-7D via polymerase chain reaction (PCR), using primer overhangs (Table S1, Supporting Information) for cloning as described in Jensen et al.^[27] STlac_7031 was built with the insertion of the *L. plantarum ldh1* (Table S4, Supporting Information) under the control of the native *TDH3* promoter for the conversion of pyruvate into lactate. Strain STmal_5413 was constructed from the TAM strain with the insertion of *MDH3* lacking the SKL mitochondrial targeting sequence (Table S4, Supporting Information), under control of the *TDH3* promoter. This gene was amplified from the genomic DNA of *S. cerevisiae* with primers PR7011 and PR7012 to amplify the region lacking the mitochondrial targeting sequence. The *S. pombe* malate transporter gene *mae1* (Table S4, Supporting Information) was also inserted under the control of the native *TEF1* promoter, along with the native *PYC1* and *PYC2* genes under the control of the native *TEF1* and *PGK1* promoters, respectively. ST $hpdh_{2779}$ and ST $hibadh_{2780}$ were engineered for 3HP production, following the designs described in Borodina et al.^[15] Native *PYC1* and *PYC2* genes were overexpressed (under the control of *TEF1* and *PGK1* promoters), along with the aspartate-1-dehydrogenase gene (*panD*) from *Tribolium castaneum* under the control of the *TEF1* promoter, and the β -alanine-pyruvate amino transferase (BAPAT) from *Bacillus cereus* (*yhxA*) under the control of the *TEF1* promoter. For the final enzymatic step of the 3HP biosynthetic pathway in ST $hpdh_{2779}$, a 3-hydroxypropionate dehydrogenase (HPDH) from *E. coli* (*ydfG*) that uses NADPH as a cofactor was expressed under the control of the *PGK1* promoter. For ST $hibadh_{2780}$, an NADH-dependent HIBADH from *Pseudomonas putida* (*hibdh*) was inserted, under the control of the *PGK1* promoter. Heterologous genes were codon-optimized and synthesized by GeneArt (Thermo Fisher Scientific, USA). The sequences of these genes can be found in the Supporting Information. Details and sequences of the genes used to create the 3HP strains can be found in Borodina et al.^[15] PCR amplification was performed on each gene, using the primers as described in Table S1, Supporting Information, with the corresponding primer overhangs to be compatible with the promoter biobricks.^[27]

The amplified promoters and genes were USER-cloned into EasyClone vectors (details of which are given in the Supporting

Table 1. Fermentation parameters of Crabtree-negative, hydroxy acid-producing strains under batch conditions.

| Strain ^{a)} | STtam_2803 | STlac_7031 | STmal_5413 | ST $hpdh_{2779}$ | ST $hibadh_{2780}$ |
|--|---------------------|-------------------|-------------------|-------------------|--------------------|
| Description | Parental TAM strain | Lactate producer | Malate producer | HPDH | HIBADH |
| Max product titers [g L^{-1}] | 16.5 ± 0.1 | 30.2 ± 2.2 | 26.8 ± 0.3 | 3.7 ± 0.1 | 3.4 ± 0.2 |
| Product yield [mol mol^{-1} glucose] | 0.340 ± 0.004 | 0.600 ± 0.091 | 0.363 ± 0.010 | 0.070 ± 0.005 | 0.067 ± 0.007 |
| Final OD ₆₀₀ | 63.9 ± 2.2 | 86.2 ± 2.4 | 58.6 ± 2.2 | 51.6 ± 0.5 | 56.5 ± 1.6 |
| Maximum specific growth rate [h^{-1}] | 0.057 ± 0.004 | 0.094 ± 0.016 | 0.058 ± 0.003 | 0.056 ± 0.008 | 0.057 ± 0.002 |
| Succinate [g L^{-1}] | 0.17 ± 0.06 | 0.42 ± 0.02 | 3.97 ± 0.08 | 0.70 ± 0.06 | 0.91 ± 0.09 |
| Glycerol [g L^{-1}] | 6.00 ± 0.05 | 0.25 ± 0.01 | 2.54 ± 0.06 | 2.07 ± 0.20 | 2.93 ± 0.18 |

^{a)}These parameters were measured in shake flask fermentations in mineral media containing 100 g L^{-1} initial glucose concentration and supplemented with 50 g L^{-1} CaCO_3 . Metabolite concentrations were analyzed by HPLC, except for malate, which was measured by enzymatic assay. Pyruvate concentration could not be quantified by HPLC for the engineered strains.

Information) digested with SfaAI (Thermo Fisher Scientific) and Nb.BsmI (New England Biolabs, USA).^[27] USER cloning (New England Biolabs) was performed as previously reported, and cloned plasmids were transformed into the *E. coli* cloning strain DH5 α via heat shock at 42 °C for one minute.^[27,28] Cells were plated on lysogeny broth (LB) agar plates with 100 $\mu\text{g mL}^{-1}$ ampicillin and incubated at 37 °C overnight. The next day, individual colonies were tested by PCR for the correctly sized plasmid insertions using the verification primers outlined in the Supporting Information. Correctness of all plasmid sequences was additionally confirmed by Sanger sequencing. Correct *E. coli* clones were stored as glycerol stocks at –80 °C and used for plasmid propagation.

Plasmids for yeast transformations were first digested with NotI (Thermo Fisher Scientific) to produce linear DNA fragments. The fragments containing expression cassettes and selection marker flanked by homologous recombination arms were purified from the vector backbone by gel electrophoresis followed by band excision and gel purification. All yeast transformations were carried out using the lithium acetate chemical transformation protocol as described in Gietz et al.^[29] After heat shock, the cells were plated directly onto synthetic the dropout agar plates. After two to three days, plates were examined for growth, and correct isolates were identified via PCR on individual colonies using the verification primers as outlined in Jensen et al.^[27]

The complete lists of strains, plasmids, biobricks, and primers used in this study are included in the Supporting Information.

2.3. Media

For the selection of *E. coli*, LB agar plates were made to contain 100 $\mu\text{g mL}^{-1}$ ampicillin. For plasmid propagation, LB broth was used with the same concentration of ampicillin.

To select *S. cerevisiae* transformants and for strain recovery from glycerol stocks, synthetic complete (SC) agar plates were prepared with premixed amino acid dropout powders, with a final glucose concentration of 20 g L^{-1} . For the creation of precultures, liquid SC media was prepared with premixed amino acid dropout powders with a final glucose concentration of 20 g L^{-1} . For the respiration experiments, the liquid complete synthetic mixture (CSM) was prepared from dropout powders purchased from Sunrise Science (USA), with 20 g L^{-1} glucose.

S. cerevisiae shake flask fermentations were performed with batch production medium optimized for acid production, prepared according to Zelle et al.^[16] with 100 g L^{-1} glucose as the carbon source.

2.4. Cultivation Conditions

For shake flask fermentation experiments, single colonies of each strain were taken from plates and inoculated into 5 mL of liquid SC medium with appropriate amino acid selection in 12 mL culture tubes and incubated at 30 °C, 250 rpm for two days. Shake flasks were prepared as follows: 5 g CaCO₃ was added to each 500 mL baffled shake flask before the flasks were autoclaved. Once cooled, 100 mL of the sterile batch production medium was added to each shake flask. The prepared flasks were inoculated from the

precultures to a starting OD₆₀₀ of 0.5. Fermentations were carried out at 30 °C, and shaking was set to 250 rpm for five days with samples taken every \approx 12 hours and measured for optical density at 600 nm in an Implen P300 spectrophotometer (dilutions were made to keep measurements within the linear range of the equipment). Part of each sample was centrifuged at 11 000 $\times g$ for five minutes, and the supernatant was stored at –20 °C until high performance liquid chromatography (HPLC) analysis. Each strain was fermented in triplicate in a shaking incubator for 120 hours at 30 °C and 250 rpm.

2.5. ¹³C-Based Metabolic Flux Analysis (MFA)

For ¹³C-based MFA, the same medium was used as in the shake flask fermentations, except that ammonia was used as the nitrogen source instead of urea; no CaCO₃ was added (to prevent nonlabeled carbon interference) and ¹³C-labeled glucose was used to a final concentration of 10 g L^{-1} . Shake flasks (250 mL) were filled with 10 mL of the medium and inoculated with the strains to a starting OD₆₀₀ of 0.06. Samples for analysis were taken once the OD₆₀₀ of the cells had reached 2.00. Cell dry weight ([CDW], 0.3 mg) was removed and washed in 0.9% NaCl before storage at –80 °C. Each strain was cultured in quadruplicate, with one culture grown on 20% U-¹³C and 80% unlabeled glucose, and the three other cultures were grown on 20% U-¹³C and 80% 1-¹³C glucose, as previously reported.^[30] Labeled glucose was purchased from Eurisotop (France). The same cultivation was performed in triplicate without labeled glucose, where samples were taken regularly during growth and measured by HPLC for the rates of secreted products, used to constrain the stoichiometric model for MFA.

The frozen cell pellets were resuspended in 150 μL of HCL (6 M) before being transferred to a silanized glass vial. The samples were left to hydrolyze at 105 °C for six hours before the remaining liquid was evaporated at 80 °C. The pellets were resuspended in 30 μL of acetonitrile. Derivatization was performed by adding *N*-methyl-*N*-tert-butylidimethylsilyl-trifluoroacetamide to a final ratio of 1:1 and incubating at 85 °C for one hour.^[31] Gas chromatography–mass spectrometry (GC–MS) analysis of the amino acid content was performed on the derivatized samples as previously reported using a TSQ 8000 XLS Triple-Quadrupole MS equipped with a PTV-injector (Thermo Fisher Scientific).^[30]

The raw GC–MS data were corrected by iMS2Flux (v7.2.1) software with default settings^[32] for natural abundance of heavy isotopes and unlabeled biomass introduced with the inoculum. Steady-state MFA was then performed with the INCA (v1.6) toolbox for MATLAB R2016b.^[33] A previously reported model metabolic network for *S. cerevisiae* was adjusted to fit the central carbon metabolism of each acid-producing strain and used as the model network input for INCA.^[34] The full list of included reactions is included in Table S5, Supporting Information. Glyoxylate cycle reactions were not included in the metabolic model due to the negligible activity when glucose is used as a substrate. Flux estimation was performed ten times with randomized initial guesses, and goodness-of-fit was assessed. The minimized residual sum of squares for each experiment was below 300. Confidence intervals (95%) of the flux parameters were calculated using the Monte Carlo method in INCA.

The metabolic fluxes estimated with INCA were used to constrain a modified version of the iMM904 genome-scale metabolic model (GEM) of *S. cerevisiae*.^[35] This model was modified by deleting the PDC reaction to eliminate ethanol production, and the heterologous pathways for each strain were added to the reactions in the model, producing a distinct model for each strain. These models were used to determine the remainder of the fluxes using parsimonious flux balance analysis implemented in the Cameo (v0.11.6) toolbox for Python 3.4.^[36,37]

2.6. Transcriptomics

For transcriptomic analysis, triplicate fermentations identical to those for the ¹³C-MFA experiments were performed with nonlabeled glucose. Once the fermentations reached the harvest OD₆₀₀ of 2, biomass samples were removed, cooled quickly on ice, and centrifuged at 4 °C for ten minutes at 5000 × g. The supernatant was removed and the pellets were snap-frozen with liquid nitrogen and stored at −80 °C until they were further processed. For RNA extraction, the RNeasy Mini Kit (Qiagen) was used, followed by treatment with DNase (RNase-Free DNase Set; Qiagen) for the digestion of residual genomic DNA. Library preparation and sequencing was performed as described previously.^[30] Mapping, alignment, and differential expression analysis were performed with the HISAT2 (v2.1.0), StringTie (v1.3.5), and DESeq. 2 (v1.22.1) in R Studio (v1.1.442).^[38–40] The false discovery rate for differential expression was controlled by the Benjamini–Hochberg method, after *p*-value estimation via the Wald significance test.^[39,41] Principal component analysis (PCA) was performed with the PCA tools within DESeq. 2. Array Express accession number was E-MTAB-7600.

2.7. Analytical Methods

Concentrations of extracellular metabolites were measured by HPLC. The supernatant was removed and transferred to Nunc 96-well plates with rubber sealing top (Thermo Fisher Scientific). Each sample of 30 μL was injected, and analytes were separated on an Aminex HPX-87H ion exclusion column (Bio-Rad, USA) at 60 °C using 5 mM H₂SO₄ as eluent with a flow rate of 600 μL min^{−1} for 30 minutes. The compounds were detected with a Dionex RI-101 Refractive Index Detector at 45 °C and a DAD-3000 Diode Array Detector at 210 nm (Dionex, USA). For analysis of 3HP, the same protocol was run except that 1 mM H₂SO₄ was used as eluent, with a longer run time of 45 minutes. Due to the overlapping spectra of pyruvate and malate in this method, malate concentrations were verified using the L-Malic Acid Assay Kit (K-LMAL-116A; Megazyme, Republic of Ireland). Pyruvate was verified using a Pyruvic Acid Assay Kit (K-PYRUV; Megazyme). Standards for analysis were purchased from Sigma-Aldrich, USA. The 3HP standard was purchased from TCI, Japan.

2.8. Respiration Monitoring

To analyze the respiration characteristics of the hydroxy acid production strains, each strain was tested in a respiration activity

monitoring system (RAMOS).^[42] Individual colonies of each strain were inoculated into 5 mL of CSM lacking the appropriate amino acids. The following day the RAMOS was calibrated and checked for correct function following the manufacturer's guidelines. The RAMOS shake flasks were inoculated to a starting OD₆₀₀ of 0.2 and set to shake at 300 rpm with the temperature set to remain constant at 30 °C. The fermentations lasted for 48 hours, with oxygen and carbon dioxide automatically measured every 30 minutes. Samples were taken for analysis and tested for optical density every ≈12 hours. Each experiment was performed in triplicate.

2.9. Statistics

The fermentation data in this study were analyzed and statistics calculated using GraphPad Prism software version 7 (GraphPad Software Inc.). Significance was calculated with Tukey's multiple comparisons test for one-way analysis of variance. All values are expressed as the mean average ± standard deviation.

2.10. Chemicals

Unless otherwise stated, all reagents and chemicals were purchased from Sigma-Aldrich, USA.

3. Results

3.1. Physiological Characterization of Hydroxy Acid-Producing PDC-Negative *S. cerevisiae*

We constructed four different hydroxy acid-producing strains, all with an evolved glucose-tolerant PDC-negative strain as the chassis, referred to as the TAM strain, which produces and excretes high levels of pyruvate.^[11] We chose three different hydroxy acids that are commonly produced from pyruvate: lactic, malic, and 3HP acids. We reconstructed previously published designs for high-level production of lactate and malate with the TAM strain.^[16,43] Two different versions of the β-alanine route to 3HP biosynthesis were constructed, each utilizing a different redox cofactor (NADH or NADPH) in the final enzymatic step of the pathway.^[15]

We performed shake flask fermentations using a batch medium composition that has previously been shown to be suitable for the production of malic acid to high titers in the TAM strain. Glucose (100 g L^{−1}) was used as the carbon source, with 50 g L^{−1} CaCO₃ added as a neutralizing agent (Figure 2 and Table 1).^[16] Growth rates, under this condition, were similar for all of the strains apart from for the lactate producer (STlac_7031), which had a significantly (*p* < 0.01) higher growth rate (0.094 ± 0.016 h^{−1}) than the parental strain STtam_2803 (0.057 ± 0.004 h^{−1}).

STlac_7031 and STmal_5413 both produced high levels of their products, with final measured lactate and malate concentrations of 30.2 ± 2.2 g L^{−1} and 26.8 ± 0.3 g L^{−1}, respectively. This was higher than the pyruvate production in the parental strain, which had a maximum titer of only 16.5 ± 0.1 g L^{−1}. SThpdh_2779 and SThbadh_2780 showed continued product formation in the

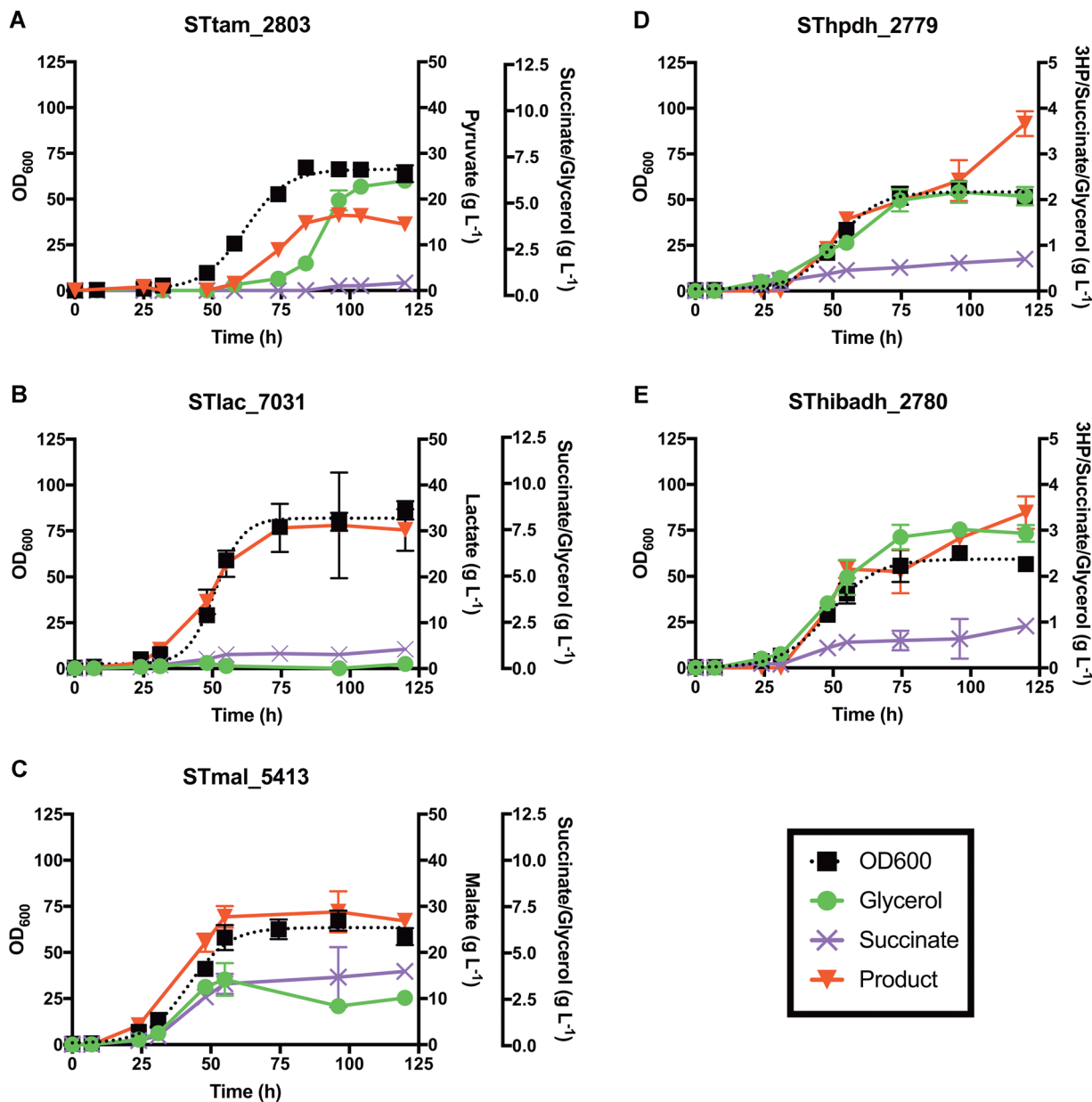


Figure 2. Fermentation profiles of the hydroxy acid production strains. Time-course fermentations with 100 g L^{-1} initial glucose concentrations showing A) STtam_2803, parental TAM strain; B) STlac_7031, TAM strain with lactate production pathway; C) STmal_5413, TAM strain with malate production pathway; D) SThpdh_2779, TAM strain with HPDH-dependent 3HP pathway; and E) SThibadh_2780, TAM strain with HIBADH-dependent 3HP pathway. Each fermentation was run for 120 hours and in triplicate. Metabolite concentrations were analyzed by HPLC, except for malate, which was measured by enzymatic assay. Pyruvate concentration could not be quantified by HPLC for the engineered strains. Values shown are the mean average for each time point \pm SD. OD, optical density.

stationary phase. The two 3HP strains produced similar levels of 3HP by the end of the fermentation, $3.7 \pm 0.13 \text{ g L}^{-1}$ and $3.4 \pm 0.17 \text{ g L}^{-1}$, respectively. STtam_2803 produced high levels of glycerol, with $\approx 6 \text{ g L}^{-1}$ measured after 120 hours. Glycerol production was lower in all of the other strains. The final C-mol yield of lactate in STlac_7031 was 25%, greater than that of malate in ST5314 ($0.30 \text{ C-mol C-mol}^{-1}$ vs $0.24 \text{ C-mol C-mol}^{-1}$ glucose), potentially due to the lower energetic requirement of lactate biosynthesis. Differences in by-product secretion were found

between the two 3HP-producing strains. Both produced similar levels of succinate ($\approx 0.8 \text{ g L}^{-1}$), but SThibadh_2780 produced 50% more glycerol than SThpdh_2779 (3 g L^{-1} and 2 g L^{-1} , respectively).

3.2. Characterization of Respiration Profiles

The RAMOS is capable of measuring both the oxygen and carbon transfer rates (OTR and CTR, respectively) during

microbial fermentations, and from this the respiratory quotients (RQs) of the strains are determined.^[42] STtam_2803 showed a tightly linked OTR and CTR through the fermentations, with an RQ of 1. All of the tested strains had near-identical OTRs during the first ten hours of fermentation. STlac_7031 was the PDC-negative strain showing the earliest slowdown of OTR, beginning at ≈ 18 hours (Figure S1, Supporting Information). However, later in the fermentation, the OTR of STlac_7031 increased again and showed two additional peaks not observed in any of the other experiments. The cause of this profile is not precisely clear, but it could be due to the consumption of pyruvate and/or lactate after the glucose has been depleted.^[44] Additionally, STlac_7031, similar to the PDC-positive strain, was able to metabolize all of the glucose with lower levels of total oxygen consumption compared to the other strains (Supporting Information).

3.3. ¹³C-Based MFA

We employed ¹³C-based MFA, combined with genome-scale modeling, to identify flux distribution differences between the production strains. Each strain was cultivated in a defined liquid batch medium containing 10 g L⁻¹ of ¹³C-labeled glucose as the carbon source.^[16] The strains were cultivated in shake flasks lacking CaCO₃ and samples were taken when each strain reached the mid-exponential phase. Once collected, samples were analyzed by GC-MS and the fluxes were calculated using the iMS2flux and INCA programs.^[32,33] The iMM904 genome-scale model of *S. cerevisiae* was constrained with the calculated fluxes to estimate the global flux distribution for each strain (Figure 3).

Using the medium without CaCO₃ resulted in higher maximum specific growth rates μ_{\max} of the strains than in the previous cultivations with 100 g L⁻¹ and CaCO₃ (Section 3.1) (Table S6, Supporting Information). STlac_7031 and STmal_5413 strains had, respectively, 64% and 20% higher μ_{\max} values than STtam_2803 while both 3HP-producing strains showed 21–26% lower rates than STtam_2803. In Table S6, Supporting Information, the secretion rates of metabolites are also presented. We succeeded in quantifying pyruvate in these cultivations using an enzymatic assay. Interestingly, pyruvate secretion rates were much lower in STlac_7031 (0.131 ± 0.016 mmol gCDW⁻¹ h⁻¹) and STmal_5413 (0.130 ± 0.026 mmol gCDW⁻¹ h⁻¹) strains than in the parental STtam_2803 strain (0.541 ± 0.106 mmol gCDW⁻¹ h⁻¹), while pyruvate secretion rates for the 3HP-producing strains were not significantly different from the parent strain.

During respiro-fermentative growth, as is expected during shake flask cultivations, fluxes through the pentose phosphate (PP) pathway and tricarboxylic acid cycle (TCA) cycle are typically low in PDC-positive WT strains.^[45,46] In contrast, all PDC-negative strains analyzed in the present study diverted most of the carbon flux (>90%) into the PP pathway. However, in a previous MFA study of a malate-producing variant of the TAM background, such a high flux in the PP pathway was not observed.^[16] Differences in the experimental conditions and methods of analysis between the two studies may explain some of the variations, but further work is required to identify the cause of the high carbon flux in the PP pathway in the strains

presented here. The flux through the TCA cycle remained low, especially in both 3HP-producing strains.

Both 3HP strains showed higher relative fluxes compared with STlac_7031 and STmal_5413 (but lower than the parental strain) in the formation of glycerol-3-phosphate from DHAP, and from the reversed transaldolase reaction: E4P + F6P → S7P + G4P. STlac_7031 and STmal_5413 kept a high proportion of their carbon flux through 3-phosphoglycerate into pyruvate, presumably due to the presence of a suitable carbon sink. From pyruvate, both 3HP strains showed flux ratios similar to STmal_5413 for oxaloacetate synthesis. SThibadh_2780 showed higher PYC flux than SThpdh_2779, but both strains showed near-identical fluxes through the aspartate amino transferase (AAT) step, with the reaction only processing around half of the flux supplied from the PYC reaction (Supporting Information).

3.4. Transcriptome Analysis

We performed an analysis of the transcriptomes of the hydroxy acid production strains to probe how the introduced pathways affect the transcriptional profile (Figure 3). STlac_7031 displayed nine transcripts that were significantly ($q < 0.05$) and highly differentially expressed (\pm twofold change), while STmal_5413 displayed 41 such transcripts, SThpdh_2779 had 23, and SThibadh_2780 had 30 (all in comparison with the TAM strain). A total of 69 highly differentially expressed transcripts were found across the strains, but none were found to be highly differentially expressed across all strains. A total of seven transcripts were highly differentially expressed across the three strains (*IRT1*, *YAR075W*, *HSP26*, *PAU15*, *DED1*, *YPR145C-A*, and *YMR175W-A*). Several of these encode proteins of unknown function, but characterized transcripts are involved in a diverse set of cellular functions including control of gametogenesis, heat-shock response, and translation initiation. Out of the 23 genes that were highly differentially expressed in SThpdh_2779, 18 of these were also found in SThibadh_2780. Several genes involved in the allantoin degradation pathway were found to be highly upregulated, which was also observed in a PDC-positive strain expressing the β -alanine pathway (unpublished results). We analyzed the variance across the strains via PCA, as shown in Figure 4. This illustrates that STlac_7031 only showed a small variance from the parental STtam_2803, while STmal_5413 showed higher variation from STtam_2803, as did SThpdh_2779 and SThibadh_2780. These latter two strains showed a small variation from one another and both were discrete from the profile of STmal_5413.

We next mapped the transcriptional profiles to the central carbon metabolism (Figure 3). STlac_7031 showed only slight differences in transcript levels over the central carbon metabolism, with small changes in the genes involved in glycerol production. The remaining strains showed greater deviation in their transcriptional abundances. STmal_5413, SThpdh_2779, and SThibadh_2780 all upregulated *HXX2*, a gene involved in the conversion of glucose into glucose-6-phosphate, the flux-controlling step of glycolysis. STlac_7031 also showed an upregulation of this step, but instead through

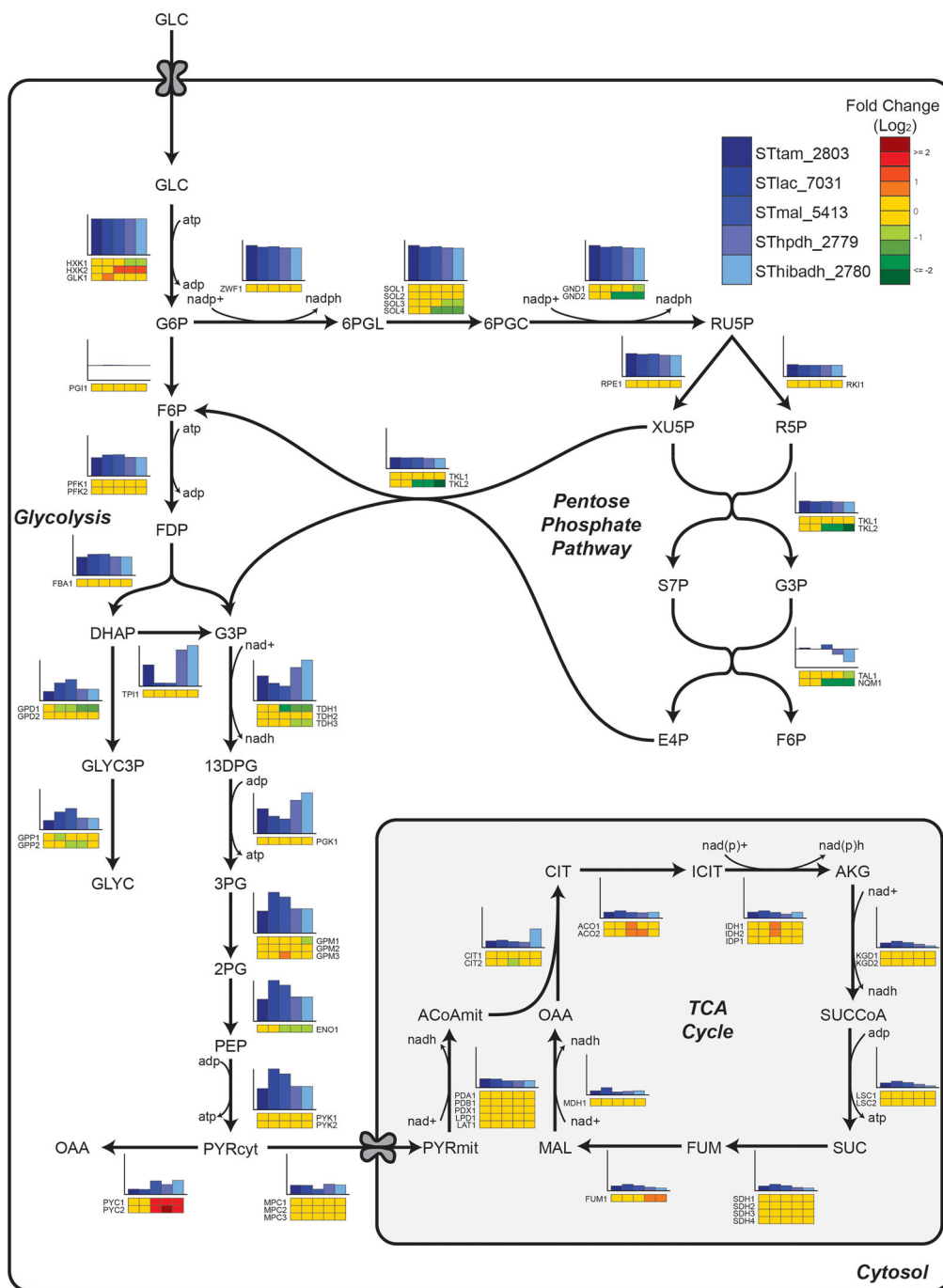


Figure 3. ^{13}C -based metabolic flux and transcriptomic analyses of central carbon metabolism of the hydroxy acid-producing strains under batch fermentation conditions with 10 g L^{-1} initial glucose concentrations. Crabtree-negative *S. cerevisiae* strains (TAM—STam_2803) producing different hydroxy acids: lactate (STlac_7031), malate (STmal_5413), and 3HP (SThpdh_2779 and SThibadh_2780) were analyzed for their relative flux distributions and the differential expression of the genes involved in each reaction. Bar charts next to each reaction show the relative flux values for each strain calculated from a genome-scale model constrained with data from ^{13}C -MFA (normalized over glucose uptake rate). Underneath each graph are heat map plots for the relative transcript levels. Beside each heat map plots are the name of the associated gene. AC, acetate; ACALD, acetaldehyde; ACoAmit, acetyl-CoA (mitochondrial); AKG, α -ketoglutarate; CIT, citrate; DHAP, dihydroxy-acetone-phosphate; 13DPG, 1,3-diphosphateglycerate; E4P, erythrose-4-phosphate; EtOH, ethanol; F6P, fructose-6-phosphate; FDP, fructose-1,6-diphosphate; FUM, fumarate; GLC, glucose; GLYC, glycerol; GLYC3P, glycerol-3-phosphate; G3P, glyceraldehyde-3-phosphate; G6P, glucose-6-phosphate; ICIT, isocitrate; MAL, malate; OAA, oxaloacetate; PEP, phosphoenolpyruvate; 2PG, 2-phosphoglycerate; 3PG, 3-phosphoglycerate; 6PGC, 6-phospho-D-gluconate; 6PGL, D-6-phospho-glucono- δ -lactone; PYRcyt, pyruvate (cytosolic); PYRmit, pyruvate (mitochondrial); RU5P, ribulose-5-phosphate; R5P, ribose-5-phosphate; SUC, succinate; SUCCoA, succinyl-CoA; S7P, sedoheptulose-7-phosphate; XU5P, xylulose-5-phosphate.

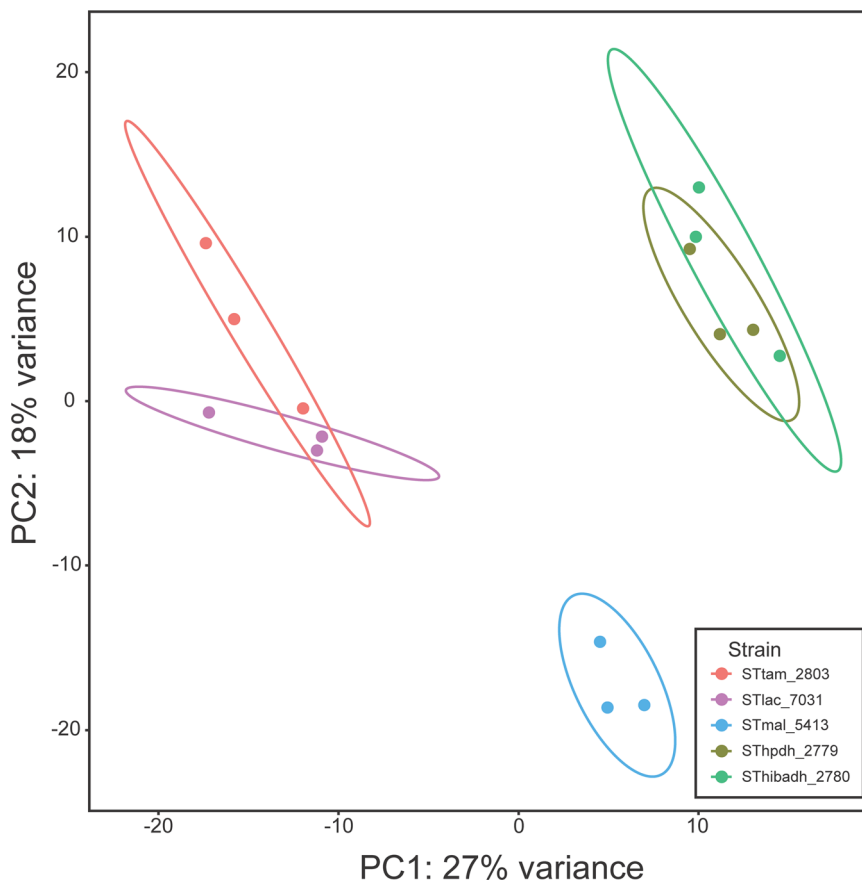


Figure 4. PCA of the transcriptomic profiles of Crabtree-negative hydroxy acid production strains. Each point represents a single biological replicate, while color denotes the strain identity. The contours of the same color represent 95% of confidence bounds for each strain. PC, principal component.

GLK1. However, only *STmal_5413* and *STlac_7031* showed higher glucose uptake rates than the parental strain (Table S5, Supporting Information). *STmal_5413*, *SThpdh_2779*, and *SThbadh_2780* all showed downregulation across parts of the PP pathway and in steps found in lower glycolysis. While TCA cycle genes did not show large transcriptional changes, *STmal_5413* experienced upregulation of the two steps required to convert citrate into α -ketoglutarate, while *SThpdh_2779* and *SThbadh_2780* experienced upregulation of *FUM1*, responsible for the conversion of fumarate to malate.

4. Discussion

In this study, we characterized hydroxy acid production in a Crabtree-negative, pyruvate-overproducing *S. cerevisiae* strain—the TAM strain. Introduction of a lactate or malate production pathway restores some of the growth defects found in the TAM strain by resupplying cytosolic NAD⁺. The energetic requirements of lactate and malate transport, combined with the mutation found in *MTH1*, prevent *STlac_7031* and *STmal_5413* from reaching the growth rate of ethanol-producing PDC-positive *S. cerevisiae*. Interestingly, although lactate production facilitated a significantly higher growth rate in *STlac_7031*, the transcriptional profile remained close to that of the parental strain, suggesting that this pathway has not

caused a dramatic shift in the regulatory mechanisms of the TAM strain. Malate production does appear to cause large changes across the regulatory mechanisms, with a significant divergence in the profile compared to the parental strain. Unlike lactate and malate production, NADH-dependent production of 3HP in *SThbadh_2780* was unable to provide any growth restoration and both 3HP-producing strains had reduced growth rates compared to *STtam_2803* when fermented in the absence of CaCO₃. A slight growth improvement of the HIBADH (*SThbadh_2780*) strain over the HPHD strain (*SThpdh_2779*) may have been expected due to *SThbadh_2780* regenerating NAD⁺ during 3HP synthesis, but no such difference between the strains was observed. Both strains showed similar transcriptional profiles across the central carbon metabolism and no difference between them was observed in the NADPH-producing PP pathway, of which both strains downregulated several genes. The lower growth rates suggest that both 3HP pathways are deleterious to the fitness of the host, perhaps due to the accumulation of 3HP aldehyde.^[47] This effect, together with the much lower titers of 3HP compared to the other hydroxy acids, may cancel any positive effects provided by NAD⁺ regeneration.

Pyruvate yields on glucose were reported in the TAM strain to be 0.92 mol mol⁻¹ glucose.^[11] In this study, we record yields of only 0.34 mol mol⁻¹ glucose. This difference is most likely

due to the repeated glucose feedings used in the previous report. We also obtained lower yields for lactate and malate production (0.60 mol mol⁻¹ vs 1.44 mol mol⁻¹ glucose for lactate production and 0.36 mol mol⁻¹ vs 0.42 mol mol⁻¹ glucose for malate production).^[16,43] The cause of this difference is likely due to the use of high-copy-number plasmids in the previous works, and only single-copy chromosomal integrations in the present study. PDC-positive *S. cerevisiae* expressing the HPDH version of the 3HP pathway produced a yield of 0.09 mol mol⁻¹ glucose in batch media conditions, slightly higher than the same pathway expressed in the TAM strain—SThpdh_2779 (0.07 mol mol⁻¹ glucose).^[15] The poorer performance of the TAM-based strains compared to the PDC-positive host is surprising and is perhaps due to the media conditions not being optimal for 3HP production. However, the 3HP titers were much higher than those previously published under batch fermentation conditions.^[15] When these 3HP pathways were expressed in a PDC-positive strain, there was a greater difference between the performance of the HPDH and HIBADH enzymes, with the strain carrying HPDH producing ≈fourfold higher titers of 3HP than a strain carrying the HIBADH enzyme.^[15] The observation that the HIBADH pathway performed relatively better in the TAM background is consistent with expectations as the PDC-negative strain exhibits an NADH imbalance.

Both SThpdh_2779 and SThibadh_2780 had similar flux into oxaloacetate as STmal_5413, suggesting that *PYC1* and *PYC2* overexpression is correctly functioning to push the flux into oxaloacetate from pyruvate in these strains. However, they are unable to channel this additional flux into 3HP production. Even though SThibadh_2780 showed higher flux than SThpdh_2779 through *PYC*, the near-identical downstream fluxes of both strains suggest that the flux-controlling step is positioned lower in the pathway. One candidate for this step is aspartate decarboxylase (*PAND*). We previously reported that increasing the copy number of *PAND*-encoding gene improved 3HP production in the PDC-positive background.^[15] Both strains also showed similar transcriptional profiles, and both showed differentially expressed genes related to allantoin degradation. Further investigation may uncover what role this pathway may be having on 3HP production via this pathway.

The impaired growth of both 3HP strains may be due in part to a toxic accumulation of malonic semialdehyde, with the detoxification by HPDH/HIBADH unable to proceed quickly enough to allow the cell to grow rapidly.^[48,49] Investigations of the transport mechanisms of 3HP from the cytosol to the extracellular space could help to pull flux from malonic semialdehyde and restore growth. Another strategy may be to engineer a malonic semialdehyde sensor to dynamically control flux through the pathway, similar to the previous work carried out on 3HP biosensors.^[50,51]

We hope that the data provided here will help to inform future attempts to engineer hydroxy acid production in PDC-negative hosts. Our findings illustrate how the fluxes are distributed in these strains, and how the different production pathways impact the transcriptional landscape. However, further work is required to identify the mechanisms behind these changes and how they may be exploited to increase the productivity of these hosts.

Supporting Information

Supporting Information is available from the Wiley Online Library or from the author.

Acknowledgements

The authors acknowledge the financial support from the Novo Nordisk Foundation (grant agreement no. NNF10CC1016517), from the European Research Council under the European Union's Horizon 2020 research and innovation programme (YEAST-TRANS project, grant agreement no. 757384), from the European Commission in the 7th Framework Programme (BioREFINE-2G project, grant agreement no. FP7-613771), and from the European Union's Horizon 2020 research and innovation programme under the Marie Skłodowska-Curie grant agreement no. 722287 (PaCMEN project). M.M.J.-F. thanks the Idella foundation for financing the research stay at Joint BioEnergy Institute, USA. L.M.B. acknowledges funding by the Cluster of Excellence "The Fuel Science Center—Adaptive Conversion Systems for Renewable Energy and Carbon Sources," which is funded by the Excellence Initiative of the German federal and state governments to promote science and research at German universities. The authors thank Prof. Jack Pronk (TU Delft) for gifting *S. cerevisiae* TAM strain and Prof. Peter Kötter, Johann Wolfgang Goethe University, Frankfurt, Germany for gifting *S. cerevisiae* strain CEN.PK113-7D.

Conflict of Interest

Irina Borodina has a financial interest in BioPhero ApS. J.D.K. has a financial interest in Amyris, Lygos, Demetrix, Constructive Biology, Maple Bio, Ansa Biotechnology, and Napigen.

Keywords

¹³C-based metabolic flux analysis, central carbon metabolism, Crabtree-negative, hydroxy acid, transcriptomics

Received: January 8, 2019

Revised: March 21, 2019

Published online: May 17, 2019

- [1] J. T. Pronk, H. Yde Steensma, J. P. Van Dijken, *Yeast* **1996**, *12*, 1607.
- [2] S. Kim, J.-S. Hahn, *Metab. Eng.* **2015**, *31*, 94.
- [3] E. Nevoigt, *Microbiol. Mol. Biol. Rev.* **2008**, *72*, 379.
- [4] M. T. Flikweert, J. P. van Dijken, J. T. Pronk, *Appl. Environ. Microbiol.* **1997**, *63*, 3399. <http://aem.asm.org/content/63/9/3399.abstract>.
- [5] O. de Smidt, J. C. du Preez, J. Albertyn, *FEMS Yeast Res.* **2008**, *8*, 967.
- [6] H. D. Schmitt, F. K. Zimmermann, *J. Bacteriol.* **1982**, *151*, 1146.
- [7] P. G. Seeboth, K. Bohnsack, C. P. Hollenberg, *J. Bacteriol.* **1990**, *172*, 678.
- [8] S. Hohmann, *J. Bacteriol.* **1991**, *173*, 7963.
- [9] M. T. Flikweert, L. van der Zanden, W. M. Janssen, H. Yde Steensma, J. P. van Dijken, J. T. Pronk, *Yeast* **1996**, *12*, 247.
- [10] M. T. Flikweert, M. de Swaaf, J. P. van Dijken, J. T. Pronk, *FEMS Microbiol. Lett.* **1999**, *174*, 73.
- [11] A. J. A. van Maris, J.-M. A. Geertman, A. Vermeulen, M. K. Groothuizen, A. A. Winkler, M. D. W. Piper, J. P. van Dijken, J. T. Pronk, *Appl. Environ. Microbiol.* **2004**, *70*, 159. <http://aem.asm.org/content/70/1/159.abstract>.
- [12] B. Oud, C.-L. Flores, C. Gancedo, X. Zhang, J. Trueheart, J.-M. Daran, J. T. Pronk, A. J. A. van Maris, *Microb. Cell Fact.* **2012**, *11*, 131.
- [13] N. Ishida, S. Saitoh, K. Tokuhira, E. Nagamori, T. Matsuyama, K. Kitamoto, H. Takahashi, *Appl. Environ. Microbiol.* **2005**, *71*, 1964. <http://aem.asm.org/content/71/4/1964.abstract>.
- [14] D. A. Abbott, R. M. Zelle, J. T. Pronk, A. J. A. van Maris, *FEMS Yeast Res.* **2009**, *9*, 1123.

- [15] I. Borodina, K. R. Kildegaard, N. B. Jensen, T. H. Blicher, J. Maury, S. Sherstyk, K. Schneider, P. Lamosa, M. J. Herrgård, I. Rosenstand, F. Öberg, J. Forster, J. Nielsen, *Metab. Eng.* **2015**, *27*, 57.
- [16] R. M. Zelle, E. de Hulster, W. A. van Winden, P. de Waard, C. Dijkema, A. A. Winkler, J.-M. A. Geertman, J. P. van Dijken, J. T. Pronk, A. J. A. van Maris, *Appl. Environ. Microbiol.* **2008**, *74*, 2766.
- [17] S. Colombié, S. Dequin, J. M. Sablayrolles, *Enzyme Microb. Technol.* **2003**, *33*, 38.
- [18] A. J. A. van Maris, W.N. Konings, J. P. van Dijken, J. T. Pronk, *Appl. Environ. Microbiol.* **2004**, *70*, 2898. <http://aem.asm.org/content/70/5/2898.abstract>.
- [19] P. Branduardi, M. Sauer, L. De Gioia, G. Zampella, M. Valli, D. Mattanovich, D. Porro, *Microb. Cell Fact.* **2006**, *5*, 4.
- [20] E. Nagamori, K. Shimizu, H. Fujita, K. Tokuhira, N. Ishida, H. Takahashi, *Bioprocess Biosyst. Eng.* **2013**, *36*, 1261.
- [21] A. J. A. van Maris, W. N. Konings, J. P. van Dijken, J. T. Pronk, *Metab. Eng.* **2004**, *6*, 245.
- [22] L. McAlister-Henn, J. S. Steffan, K. I. Minard, S. L. Anderson, *J. Biol. Chem.* **1995**, *270*, 21220. <http://www.jbc.org/content/270/36/21220.abstract>.
- [23] C. Camarasa, F. Bidard, M. Bony, P. Barre, S. Dequin, *Appl. Environ. Microbiol.* **2001**, *67*, 4144. <http://aem.asm.org/content/67/9/4144.abstract>.
- [24] M. Casal, S. Paiva, O. Queirós, I. Soares-Silva, *FEMS Microbiol. Rev.* **2008**, *32*, 974.
- [25] T. Zambanini, W. Kleineberg, E. Sarikaya, J. M. Buescher, G. Meurer, N. Wierckx, L. M. Blank, *Biotechnol. Biofuels* **2016**, *9*, 135.
- [26] V. Kumar, S. Ashok, S. Park, *Biotechnol. Adv.* **2013**, *31*, 945.
- [27] N. B. Jensen, T. Strucko, K. R. Kildegaard, F. David, J. Maury, U. H. Mortensen, J. Forster, J. Nielsen, I. Borodina, *FEMS Yeast Res.* **2014**, *14*, 238.
- [28] H. H. Nour-Eldin, F. Geu-Flores, B. A. Halkier, *Methods Mol. Biol.* **2010**, *643*, 185.
- [29] R. D. Gietz, R. H. Schiestl, *Nat. Protoc.* **2007**, *2*, 31.
- [30] K. R. Kildegaard, N. B. Jensen, K. Schneider, E. Czarnotta, E. Ozdemir, T. Klein, J. Maury, B. E. Ebert, H. B. Christensen, Y. Chen, I.-K. Kim, M. J. Herrgard, L. M. Blank, J. Forster, J. Nielsen, I. Borodina, *Microb. Cell Fact.* **2016**, *15*, 53.
- [31] A. Schmitz, B. E. Ebert, L. M. Blank, in *GC-MS-Based Determination of Mass Isotopomer Distributions for ¹³C-Based Metabolic Flux Analysis* (Eds: T. J. McGenity, K. N. Timmis, B. Nogales), Springer, Berlin, Heidelberg **2017**, pp. 223–243. doi:10.1007/8623_2015_78.
- [32] C. H. Poskar, J. Huege, C. Krach, M. Franke, Y. Shachar-Hill, B. H. Junker, *BMC Bioinf.* **2012**, *13*, 295.
- [33] J. D. Young, *Bioinformatics* **2014**, *30*, 1333.
- [34] T. M. Wasylenko, G. Stephanopoulos, *Biotechnol. Bioeng.* **2015**, *112*, 470.
- [35] M. L. Mo, B. O. Palsson, M. J. Herrgard, *BMC Syst. Biol.* **2009**, *3*, 37.
- [36] J. G. R. Cardoso, K. Jensen, C. Lieven, A. S. Lærke Hansen, S. Galkina, M. Beber, E. Özdemir, M. J. Herrgård, H. Redestig, N. Sonnenschein, *ACS Synth. Biol.* **2018**, *7*, 1163.
- [37] N. E. Lewis, K. K. Hixson, T. M. Conrad, J. A. Lerman, P. Charusanti, A. D. Polpitiya, J. N. Adkins, G. Schramm, S. O. Purvine, D. Lopez-Ferrer, K. K. Weitz, R. Eils, R. König, R. D. Smith, B. Ø. Palsson, *Mol. Syst. Biol.* **2010**, *6*, 390.
- [38] M. Perteua, D. Kim, G. M. Perteua, J. T. Leek, S. L. Salzberg, *Nat. Protoc.* **2016**, *11*, 1650.
- [39] M. I. Love, W. Huber, S. Anders, *Genome Biol.* **2014**, *15*, 550.
- [40] D. Kim, B. Langmead, S. L. Salzberg, *Nat. Methods* **2015**, *12*, 357.
- [41] Y. Benjamini, Y. Hochberg, *J. R. Stat. Soc. Ser. B* **1995**, *57*, 289. <http://www.jstor.org/stable/2346101>.
- [42] T. Anderlei, W. Zang, M. Papaspyrou, J. Büchs, *Biochem. Eng. J.* **2004**, *17*, 187.
- [43] C. Lui, J. Lievense, Lactic acid producing yeast—US Patent application 20050112737, **2005**.
- [44] A. Pacheco, G. Talaia, J. Sa-Pessoa, D. Bessa, M. J. Goncalves, R. Moreira, S. Paiva, M. Casal, O. Queiros, *FEMS Yeast Res.* **2012**, *12*, 375.
- [45] A. K. Gombert, M. Moreira dos Santos, B. Christensen, J. Nielsen, *J. Bacteriol.* **2001**, *183*, 1441. <http://jb.asm.org/content/183/4/1441.abstract>.
- [46] H. Maaheimo, J. Fiaux, Z. P. Cakar, J. E. Bailey, U. Sauer, T. Szyperski, *Eur. J. Biochem.* **2001**, *268*, 2464.
- [47] K. R. Kildegaard, B. M. Hallstrom, T. H. Blicher, N. Sonnenschein, N. B. Jensen, S. Sherstyk, S. J. Harrison, J. Maury, M. J. Herrgard, A. S. Juncker, J. Forster, J. Nielsen, I. Borodina, *Metab. Eng.* **2014**, *26*, 57.
- [48] M. P. Dalwadi, J. R. King, N. P. Minton, *J. Math. Biol.* **2018**, *77*, 165.
- [49] K.-S. Kim, J. G. Pelton, W. B. Inwood, U. Andersen, S. Kustu, D. E. Wemmer, *J. Bacteriol.* **2010**, *192*, 4089.
- [50] E. K. R. Hanko, N. P. Minton, N. Malys, *Sci. Rep.* **2017**, *7*, 1724.
- [51] J. K. Rogers, G. M. Church, *Proc. Natl. Acad. Sci. U. S. A.* **2016**, *113*, 2388. <http://www.pnas.org/content/113/9/2388.abstract>.